

# Immediate Impact of Acute Elevation of Intraocular Pressure on Cortical Visual Motion Processing

Nini Yuan,<sup>1,2</sup> Mengwei Li,<sup>1</sup> Xiaoxiao Chen,<sup>1</sup> Yiliang Lu,<sup>2</sup> Yuan Fang,<sup>2,5</sup> Hongliang Gong,<sup>2,5</sup> Liling Qian,<sup>2</sup> Jihong Wu,<sup>1,3,4</sup> Shenghai Zhang,<sup>1,3,4</sup> Stewart Shipp,<sup>2</sup> Ian Max Andolina,<sup>2</sup> Xinghuai Sun,<sup>1,3,4</sup> and Wei Wang<sup>2,5,6</sup>

<sup>1</sup>Department of Ophthalmology and Visual Science, Eye, Ear, Nose and Throat Hospital, Shanghai Medical College of Fudan University, Shanghai, China

<sup>2</sup>Institute of Neuroscience, The Center of Excellence in Brain and Intelligence Technology, State Key Laboratory of Neuroscience, Key Laboratory of Primate Neurobiology, Chinese Academy of Sciences, Shanghai, China

<sup>3</sup>NHC/ Chinese Academy of Medical Sciences Key Laboratory of Myopia (Fudan University), and Shanghai Key Laboratory of Visual Impairment and Restoration (Fudan University), Shanghai, China

<sup>4</sup>State Key Laboratory of Medical Neurobiology, Institutes of Brain Science and Collaborative Innovation Center for Brain Science, Fudan University, Shanghai, China

<sup>5</sup>School of Future Technology, University of Chinese Academy of Science, Beijing, China

<sup>6</sup>Shanghai Center for Brain and Brain-Inspired Intelligence Technology, Shanghai, China

Correspondence: Xinghuai Sun, Department of Ophthalmology and Visual Science, Eye, Ear, Nose and Throat Hospital, Shanghai Medical College of Fudan University, 83 Fenyang Road, Shanghai 200031, China;

[xhsun@shmu.edu.cn](mailto:xhsun@shmu.edu.cn).

Wei Wang, Institute of Neuroscience, The Center of Excellence in Brain and Intelligence Technology, State Key Laboratory of Neuroscience, Key Laboratory of Primate Neurobiology, Chinese Academy of Sciences, 320 Yueyang Road, Shanghai 200031, China;

[w.wang@ion.ac.cn](mailto:w.wang@ion.ac.cn).

NY and ML contributed equally to the work.

**Received:** October 11, 2019

**Accepted:** February 10, 2020

**Published:** May 27, 2020

Citation: Yuan N, Li M, Chen X, et al. Immediate impact of acute elevation of intraocular pressure on cortical visual motion processing. *Invest Ophthalmol Vis Sci.* 2020;61(5):59. <https://doi.org/10.1167/iovs.61.5.59>

**PURPOSE.** To physiologically examine the impairment of cortical sensitivity to visual motion during acute elevation of intraocular pressure (IOP).

**METHODS.** Motion processing in the cat brain is well characterized, its X and Y cell visual pathways being functionally analogous to parvocellular and magnocellular pathways in primates. Using this model, we performed ocular anterior chamber perfusion to reversibly elevate IOP over a range from 30 to 90 mm Hg while monitoring cortical activity with intrinsic signal optical imaging. Drifting random-dot fields and gratings were used to characterize cortical population responses to motion direction and orientation in early visual areas 17 and 18.

**RESULTS.** We found that acute IOP elevations at 50 mm Hg and above, which is often observed in acute glaucoma, suppressed cortical motion direction responses. This suppression was more profound in area 17 than in area 18, and more profound in central than peripheral visual field (eccentricities 0°–4° vs. 4°–8°) within area 17. In addition, orientation responses were more suppressed than motion direction responses for the same IOP modulation.

**CONCLUSIONS.** In contrast to human chronic glaucoma that may cause greater dysfunction in large-cell magnocellular than in small-cell parvocellular visual pathways, our direct measurement of cortical processing networks implies that the small X-cell pathway shows greater vulnerability to acute IOP elevation than the large Y-cell pathway in visual motion processing. The results demonstrate that fine discrimination mechanisms for motion in the central visual field are particularly impacted by acute IOP attacks, suggesting a neural basis for immediate visual deficits in the fine motion perception of acute glaucoma patients.

**Keywords:** glaucoma, cortical motion responses, acute intraocular pressure, optical imaging, direction and orientation map

Glaucoma, characterized by progressive optic nerve loss and visual field defects, is the leading cause of irreversible blindness worldwide.<sup>1–4</sup> Glaucoma patients suffering from chronic intraocular pressure (IOP) elevation show substantial visual deficits in motion perception, on a par with loss of form and color vision.<sup>5</sup> The motion impairments were detected both in peripheral and central visual fields.<sup>6–9</sup> This abnormal motion perception may contribute to known mobility and navigation problems for glaucoma patients, such as greater risk of falls and poorer driving performance.<sup>10</sup> However, for primary angle-closure glau-

coma, which is characterized by sudden elevated IOP and has higher prevalence in Asia,<sup>3</sup> how motion perception is affected remains unclear.

Clinically, during the acute attack stage of primary angle-closure glaucoma, IOP can be sharply elevated to 70 mm Hg and higher as a result of complete angle closure. The eye suffering an acute attack usually presents with multiple concurrent complications, such as corneal edema and cataract. This causes optic opacity that adversely affects the evaluation of visual function.<sup>3,11,12</sup> Therefore clinical measurement of visual deficits in motion perception is

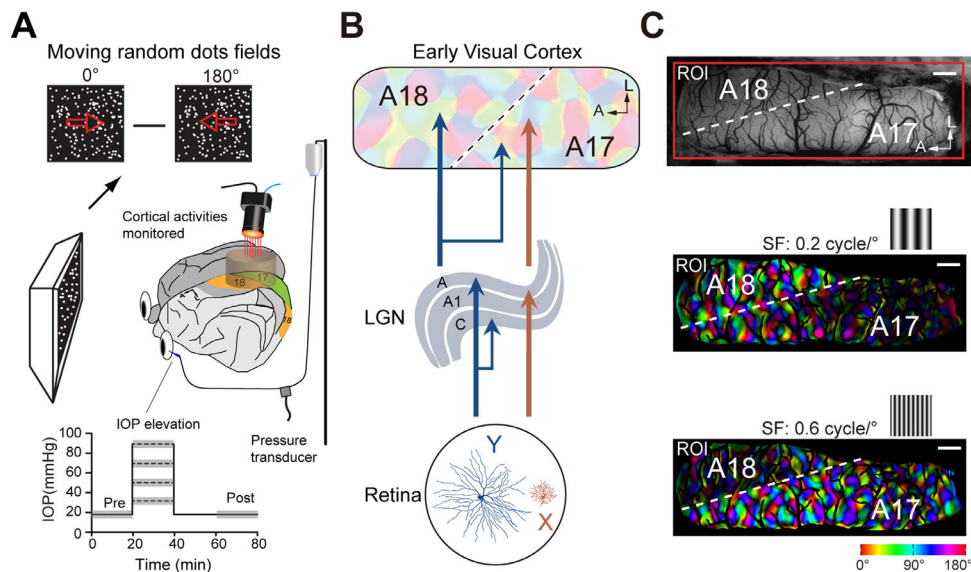


**FIGURE 1.** Experimental paradigm and parallel motion processing of cortical areas 17 and 18. **(A)** Experimental setup. IOP elevations were conducted acutely and reversibly by anterior ocular-chamber perfusion with irrigating solution, while population activities of primary visual areas 17 and 18 were monitored to motion stimuli. **(B)** Schematic illustration of the X and Y pathways in the retina, LGN, and early visual cortex.<sup>14,20–22</sup> Retinal  $\alpha$  (Y) and  $\beta$  (X) ganglion cells provide inputs to laminae A, A1, and C of the LGN, which then provides differential input into the cortex of areas 17 (X dominated) and 18 (Y dominated). **(C)** The border of cortical areas 17 and 18 was delineated by polar maps of orientation preference derived from sine-wave grating stimuli with spatial frequencies of 0.2 cycle/deg and 0.6 cycle/deg. The white broken line delimits the border between areas 17 and 18. A17, area 17; A18, area 18; A, anterior; L, lateral; ROI, region of interest; SF, spatial frequency. Scale bar: 1 mm.

difficult to perform in acute glaucoma patients. Motion is a powerful stimulus and it is only in the visual cortex that a subpopulation of neurons develop pronounced selectivity to the direction of stimulus motion. These neurons form regular and spatially organized clusters according to their preferred direction and can be quantified into a “direction map” using functional brain imaging techniques, such as intrinsic signal optical imaging.<sup>13,14</sup> Thus physiological assessment of cortical population responses to motion direction offers a means for experimental examination of motion impairments in response to acute IOP elevation.

The present study aims to characterize the impact of elevated IOP on visual motion function. Using anterior chamber perfusion with irrigating solutions for a short duration, we conducted IOP elevations equivalent to an acute attack of primary angle-closure glaucoma (Fig. 1A). The cat is one of the best studied models for visual motion processing, and its X and Y cell visual pathways are viewed as broadly equivalent to parvocellular and magnocellular pathways in primates. Visual areas 17 and 18 in the cat are analogous to the primary and secondary visual cortex (V1 and V2) in primates, although subcortical X- and Y-cell projections to both areas 17 and 18 are different compared with the primate in which combined magnocellular and parvocellular inputs dominate V1 alone. Subcortical X cells mainly project to area 17, whereas Y cells target area 18 (Fig. 1B). Using intrinsic signal optical imaging of areas 17 and 18, population responses to moving directions of random dots were recorded. As a predator, the cat has excellent visual motion discrimination. Direction maps are prominent in the early visual cortex of cats, being present in both areas 17 and 18,<sup>13–18</sup> whereas they remain undetected in V1 of primates and are limited to sparse domains in V2.<sup>19</sup> We found that acute elevation of IOP depressed the expression of direction maps. The effect was more severe in area 17 than in area 18, and in central visual field (eccentricities 0°–4°) than

in paracentral visual field (eccentricities 4°–8°) within area 17. In addition, motion direction responses were observed to be less affected than orientation responses under the same IOP modulation. Our results provide evidence that X and Y retino-geniculo-cortical pathways are differentially impacted by acute IOP elevation, with the implication that similar pathophysiology would provoke equivalent visual deficits in the motion perception of acute glaucoma patients.

## METHODS

### Animal Preparation and Maintenance

Acute experiments were performed in 12 adult cats (*Felis catus*, 6 males and 6 females, aged 1–3 years, weighted 3.1–5.0 kg). All cats were examined with an ophthalmoscope prior to experimentation to avoid retinal pathologies. All surgical and experimental procedures were in accordance with the ARVO Statement for the Use of Animals in Ophthalmic and Vision Research and approved by the Animal Care Committee of Eye and ENT Hospital of Fudan University (Shanghai, China).

Anesthesia was induced with ketamine hydrochloride (HCl; 25 mg/kg, intramuscularly [IM]) for tracheal and venous cannulation, followed by isoflurane (2.5%–5% in 70:30 N<sub>2</sub>O:O<sub>2</sub>) during subsequent surgical procedures. Atropine sulfate (1 mg, IM), dexamethasone (5 mg, IM), and gentamycin sulfate (40 mg, IM) were administered before surgery and every 12 hours throughout the experiment. The corneas were covered with carbomer ophthalmic gel (0.2%) to avoid drying immediately after anesthesia was induced, and all surgical wounds were infused with 0.5% lidocaine. Electrocardiography, respiratory rate, oxygen saturation, and expired CO<sub>2</sub> were monitored throughout the surgery and the subsequent experiment. Expired CO<sub>2</sub> was maintained at approximately 4%, and rectal temperature was kept at

38°C. After tracheal and venous cannulation, the animal was mounted in a stereotaxic frame, with a long-acting anesthetic (2% lidocaine-HCl jelly) applied to all pressure points. Craniotomy and durotomy were performed at Horsley-Clarke coordinates A6-P10, L0-L6 to expose visual cortical areas 17 and 18. A stainless steel chamber was secured on the skull using dental cement, filled with warm silicon oil (DMPS-5X; Sigma-Aldrich Corp., St. Louis, MO, USA), and sealed with a glass window as described elsewhere.<sup>14,23</sup> To monitor the blood pressure (BP) continuously, a femoral arterial cannulation was performed and connected to a pressure sensor transducer (systolic BP:  $148 \pm 18$  mm Hg; diastolic BP:  $97 \pm 13$  mm Hg; mean  $\pm$  SD,  $N = 12$  cats; Smith Medical ASD, Dublin, OH, USA).

Subsequent anesthesia and paralysis were established with isoflurane (0.5%–0.75% in 70:30 N<sub>2</sub>O:O<sub>2</sub>) and continuous infusion of gallamine triethiodide (10 mg/kg/h). Supplemental fluids (sodium lactate Ringer's solution and 5% dextrose, intravenously) were administered, approximately 50 mL every 12 hours, adjusted based on urinary output. Eyedrops containing tropicamide and Neo-Synephrine (Santen Pharmaceutical Cor., Ltd., Osaka, Japan) were applied periodically to dilate pupils and retract nictitating membranes. Contact lenses were fitted to protect the corneas, and the base curves of contact lenses were selected using streak retinoscopy to ensure that the eyes were focused on the stimulus plane. The retinae were back projected on a tangent screen placed 57 cm in front of the animal, and the positions of the area centralis were estimated from the locations of the optic disks. Experiments typically lasted 4 to 5 days, during which the optical quality of the eyes and contact lenses were checked frequently to avoid opacity or refractive error.

### Elevation of IOP

To both obtain and manipulate the IOP of an eye, a 27-gauge needle connected with a cannula filled with ionic-balanced intraocular irrigating solution (SINQI Pharmaceutical Corp., Shenyang, China) was inserted into the anterior chamber through the corneoscleral limbus. The cannula led to a three-way switch, and then to a height-adjustable reservoir containing irrigating solution for IOP manipulation, or to a pressure transducer for digital IOP display. The IOP readout immediately after anterior chamber penetration was used as the baseline IOP level for each eye ( $16 \pm 2$  mm Hg; mean  $\pm$  SD,  $N = 24$  eyes). To avoid severe retinal ischemia, which may lead to quick cell death,<sup>24</sup> a range of acute IOP elevations lower than diastolic BP (30, 50, 70, and 90 mm Hg) were achieved in a stepwise manner, each lasting for short period of approximately 20 minutes, with recovery periods of 20 minutes interleaved (Fig. 1A). Throughout the experiment, the manipulated eyes were routinely examined by ophthalmoscopes. During the transient IOP elevation, no corneal edema, cataract, or refractive errors were observed by ophthalmoscope examinations in the manipulated eyes.

### Visual Stimuli

Computer-controlled visual stimuli were displayed on a CRT monitor (1280  $\times$  960 pixels, 100 Hz, Sony Trinitron Multi-scan G520, Tokyo, Japan) covering 40°  $\times$  30° of visual angle, placed 57 cm in front of the animal's eyes. The gamma of the monitor was corrected by using the color calibration device (ColorCAL) from Cambridge Research Systems (Rochester,

UK). Visual stimuli were computer-generated using custom software based on Psychtoolbox-3 (Psychtoolbox-3 is a software package downloaded from <http://psychtoolbox.org/>). To delineate the border of area 17 with area 18, drifting sine-wave gratings with spatial frequencies of 0.6 cycles/deg and 0.2 cycles/deg (temporal frequency 3 Hz, contrast 100%), moving back and forth, were displayed perpendicularly (e.g., 0° and 90°) to map differential cortical orientation responses (Fig. 1B, 1C). Full-field displays of drifting random dots were used to activate direction maps in both areas 17 and 18 (dot diameter 0.4°, density approximately 1.1 dots per square degree, velocity 20°/s). Direction preference maps were obtained by stimulation at 30° intervals, and differential maps by contrasting responses to opposite directions (0° vs. 180° and 90° vs. 270°). To obtain the retinal eccentricity representation for areas 17 and 18, horizontal and vertical moving bars were displayed for phase response analysis (bar width 0.5°, temporal frequency 0.083 cycles/s).<sup>25</sup>

### Optical Imaging and Image Analysis

Optical imaging was performed unilaterally in a cerebral hemisphere randomly selected for each cat as previously reported.<sup>14,23,26</sup> A Dalsa Pantera 1M60 CCD camera (Waterloo, Ontario, Canada) combined with a Telecentric 55 mm f2.8 video lens (Tokyo, Japan) was used to simultaneously record both areas 17 and 18 over a certain region of interest. A 550 nm (green) illumination was used to map blood vessels, and 630 nm light (red) for intrinsic signal imaging. For each trial, two paired stimulus conditions were sequentially displayed. For example, sine-wave gratings with 0° and 90° orientations or random-dot stimuli with 0° and 180° directions were used to discriminate orientation and direction maps, respectively. The visual response for each stimulus condition was recorded for a period of 8 seconds, including 1 second before stimulus onset, and the interstimulus interval was 13 seconds. For each recording session, 32 trials were repeatedly displayed, taking a period of approximately 20 minutes.

For each stimulus condition, the recorded frames taken 2 to 6 seconds after the stimulus onset were averaged, and in turn divided by a blank frame (the average response for the 1 second before stimulus onset) to generate a single-condition map of reflectance change ( $\Delta R/R$ ). To obtain a differential orientation or direction map, the two single-condition maps within a trial were subtracted. To reduce the noise associated with blood vessels, a mask was created based on cross-trial variability calculation and modified empirically by hand according to the blood vessels mapped under 550 nm (green) illumination. Pixels within the mask were excluded in subsequent quantitative analysis. The images were then high-pass filtered (1.1–1.2 mm in diameter) and smoothed (106–306 mm in diameter) by circular averaging filters to suppress low- and high-frequency noise while avoiding signal distortion. To quantify the response amplitude, responsive patches in a differential map were defined as pixels being 1.5 SD above baseline, and the absolute  $\Delta R/R$  values in each responsive patch (i.e., including patches preferring either the first or the second condition) were averaged. This averaged intensity was taken as the measure of response amplitude. Orientation and direction preference maps were constructed using a vector summation algorithm with visual stimuli of multiple orientations (0°–180°) and directions (0°–360°) at 30° intervals.<sup>14,23</sup> The retinal eccentricity map was obtained as described in previous studies.<sup>25</sup>

## Statistical Analysis

Statistical comparisons of visual responses were performed on data compiled across cases (according to the tested eye, not the individual cat) using SPSS version 20.0 (IBM Corp., Armonk, NY, USA). One-way ANOVA was used to compare the direction responses among control IOP conditions. Paired *t*-tests were used for the following comparisons: the response amplitudes of direction maps between control and each elevated IOP condition, and the cortical response ratios during IOP elevation between different retinal eccentricities within area 17. Independent *t*-test was used for the comparison of cortical response ratios during IOP elevation between areas 17 and 18. The significance level was set at 0.05 (two-tailed).

## RESULTS

### High IOP Elevation Differentially Impacts Cortical Population Responses to Motion Direction in Areas 17 and 18

To examine the impact of different IOP levels on cortical responses to motion, we performed acute, stepwise IOP elevations (30, 50, 70, and 90 mm Hg), which range from a clinically moderate level to a level close to the diastolic BP.<sup>27</sup> Cortical population responses were recorded during monocular visual stimulation using intrinsic signal optical imaging before, during, and after acute IOP elevations. To simultaneously measure the direction selective responses in cat areas 17 and 18 (Fig. 2A), a pair of random dot fields (0°–180°) (Fig. 2B) drifting in opposite directions at a speed of 20°/s were presented sequentially.<sup>14</sup> As expected, the differential cortical population response to opposite directions was gradually reduced by increasing levels of IOP. Note that the response pattern itself was not obviously affected by acute IOP elevation, only its magnitude, as shown by the decreasing contrast of light and dark patches in the differential maps of motion direction (Fig. 2C). Direction selective response curves (Fig. 2D) quantify how response amplitude, but not preferred direction, was affected by elevated IOP.

The case presented in Figure 3 compares a pair of differential maps: one obtained for opposite horizontal directions, and one for opposite vertical directions (Figs. 3A–C). Again, the response magnitudes decrease as IOP increases (Figs. 3D, 3E), but each direction map retains its pattern, showing that IOP elevation has no impact on cortical motion direction selectivity in either areas 17 or 18. Note also that the activation achieved by vertical and horizontal motion appears about equal, as there is no difference in response magnitudes across the pair of differential maps (area 17: control:  $P = 0.18$ , 30 mm Hg:  $P = 0.06$ , 50 mm Hg:  $P = 0.40$ , 70 mm Hg:  $P = 0.093$ , 90 mm Hg:  $P = 0.17$ ; area 18: control:  $P = 0.63$ , 30 mm Hg:  $P = 0.14$ , 50 mm Hg:  $P = 0.91$ , 70 mm Hg:  $P = 0.28$ , 90 mm Hg:  $P = 0.88$ ;  $N = 16$  eyes; paired *t*-test). Averaging the response magnitudes to 0° versus 180° directions across 16 eyes (both eyes from 6 cats, and 4 eyes from the other 4 cats), we found that elevation of IOP by 30 mm Hg had no effect on either areas 17 or 18 (Fig. 3F). At higher levels of IOP, 50 mm Hg and above, there was a progressive decline in response magnitude compared with the control condition (area 17: 30 mm Hg:  $P = 0.12$ , 50 mm Hg:  $P = 9.6E-07$ , 70 mm Hg:  $P = 2.9E-07$ , 90 mm Hg:  $P = 4.0E-07$ ; area 18: 30 mm Hg:  $P = 0.90$ , 50 mm Hg:  $P = 2.8E-$

06, 70 mm Hg:  $P = 1.7E-06$ , 90 mm Hg:  $P = 8.1E-07$ ;  $N = 16$ ; paired *t*-test).

In the cat visual system, both visual areas 17 and 18 receive direct innervation from lateral geniculate nucleus (LGN), but with different proportions of X and Y pathway-specific inputs, X afferents being directed predominantly to area 17 (Fig. 1B).<sup>28,29</sup> To further compare the impact of acute IOP elevation on motion responses between areas 17 and 18, we calculated the response ratio between each IOP elevation and the control condition. At high elevated IOP levels (70 and 90 mm Hg), the response ratios revealed greater response decrements in area 17 than in area 18 (30 mm Hg:  $P = 0.54$ ; 50 mm Hg:  $P = 0.10$ ; 70 mm Hg:  $P = 0.02$ ; 90 mm Hg:  $P = 0.03$ ;  $N = 16$ ; independent *t*-test; Fig. 3G). Given that both X and Y afferents respond well to moving texture of the nature of our dot stimulus under an equivalent state of anesthesia,<sup>30,31</sup> these results suggest that the X pathway is significantly more sensitive to IOP elevation than the Y pathway.

### The Effects of Acute IOP Elevations on Cortical Direction Responses at Different Retinal Eccentricities

Clinically, the motion sensitivity of glaucoma patients is assessed perimetrically to distinguish foveal and peripheral function.<sup>32,33</sup> In cat visual cortex, as in other species, neurons are organized retinotopically according to the eccentricities of their receptive fields.<sup>34–36</sup> The smaller the eccentricity, the better the visual acuity.<sup>37</sup> If high IOP elevation has a differential effect on X and Y pathways, it may not act uniformly across the cortical retinotopic map. To examine this possibility, we used oriented bar stimuli to generate cortical eccentricity maps.<sup>25</sup> A typical example for areas 17 and 18 is shown in Figures 4A and 4B. Based on such eccentricity maps, we divided both areas 17 and 18 into central and paracentral divisions, 0° to 4° and 4° to 8°, respectively (Fig. 4C); as not all cortical exposures offered this field of view, eccentricity data were obtained from 12 eyes. To compare the impact of IOP elevation on the two eccentricity divisions, the average responses were measured at each elevated IOP level in both areas 17 and 18. For area 17 we found that, except for 30 mm Hg, higher IOPs (50, 70, and 90 mm Hg) always suppressed direction responses more in the central than the paracentral region (30 mm Hg:  $P = 0.48$ , 50 mm Hg:  $P = 1.0E-04$ , 70 mm Hg:  $P = 7.1E-03$ , 90 mm Hg:  $P = 5.6E-03$ ; paired *t*-test; Fig. 4D). In area 18, by contrast, there was no significant difference in response between central and paracentral visual fields (30 mm Hg:  $P = 0.65$ , 50 mm Hg:  $P = 0.79$ , 70 mm Hg:  $P = 0.26$ , 90 mm Hg:  $P = 0.14$ ;  $N = 12$ ; paired *t*-test; Fig. 4D). The differences across eccentricity within area 17 carry implications for the effect of acute IOP elevation on motion acuity (see Discussion).

### The Differential Effects of Acute IOP Elevations on Cortical Direction and Orientation Responses

A previous study of cat area 17 has reported that acute IOP elevation significantly decreased the cortical orientation responses to sine-wave gratings (60–110 mm Hg, 4 minutes).<sup>27</sup> Motion direction and contour orientation are two well-documented parameters of visual function, and it remains to be established whether high IOP elevation has a differential impact on these two visual features. We

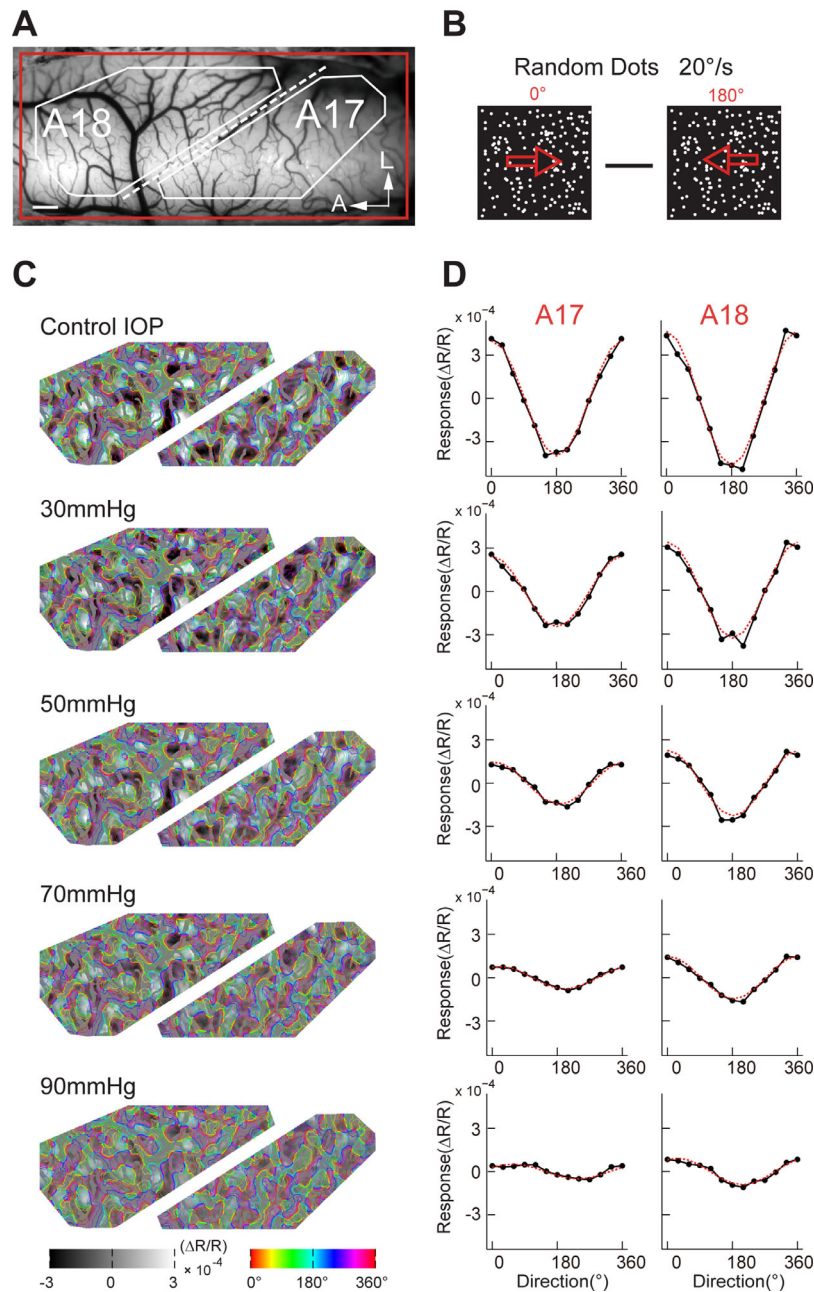


**FIGURE 2.** Example cortical direction maps in areas 17 and 18 during different levels of acute IOP elevation. **(A)** The cortical surface displaying areas 17 and 18 and the regions of interest (*white boxes*) for quantitative analysis. The *white dashed line* indicates the border of areas 17 and 18. A17, area 17; A18, area 18; A, anterior; L, lateral. *Scale bar*, 1 mm. **(B)** Stimuli of random dots drifted at 0° and 180° directions were used to elicit cortical direction maps (dots diameter 0.4°, density  $\sim 1.1$  dots per degree squared, velocity 20°/s). **(C)** Comparison of population responses across different levels of IOP elevation (30, 50, 70, and 90 mm Hg). Colored iso-direction contours were derived from direction preference maps and were superimposed onto the grayscale differential direction maps. The gray intensity scale bar here and in subsequent figures represents the response strength of intrinsic optical signals measured as the illumination reflectance change ( $\Delta R/R$ ). **(D)** The direction selective response curves derived from the population responses in (C).

thus directly compared the effect of acute IOP elevation on cortical motion direction and orientation responses in the same preparation. Using an elevated IOP level of 70 mm Hg, which is frequently observed during the acute attack phase in angle-closure glaucoma, the cortical population responses to grating orientation were assessed in six cats. As shown in [Figure 5](#), this IOP elevation suppressed the differential response to grating orientation more than the differential response to motion direction in both areas 17

and 18 ([Figs. 5C, 5D](#)). Average responses across eight eyes (both eyes from two cats, and four eyes from the other four cats) showed that the direction response ratios (with respect to control) were consistently larger than orientation response ratios during acute IOP elevation (area 17:  $P = 5.0E-04$ ; area 18:  $P = 1.2E-03$ ;  $N = 8$  eyes; paired *t*-test; [Fig. 5E](#)). This result indicates that acute high IOP elevation may affect visual form more adversely than visual motion.

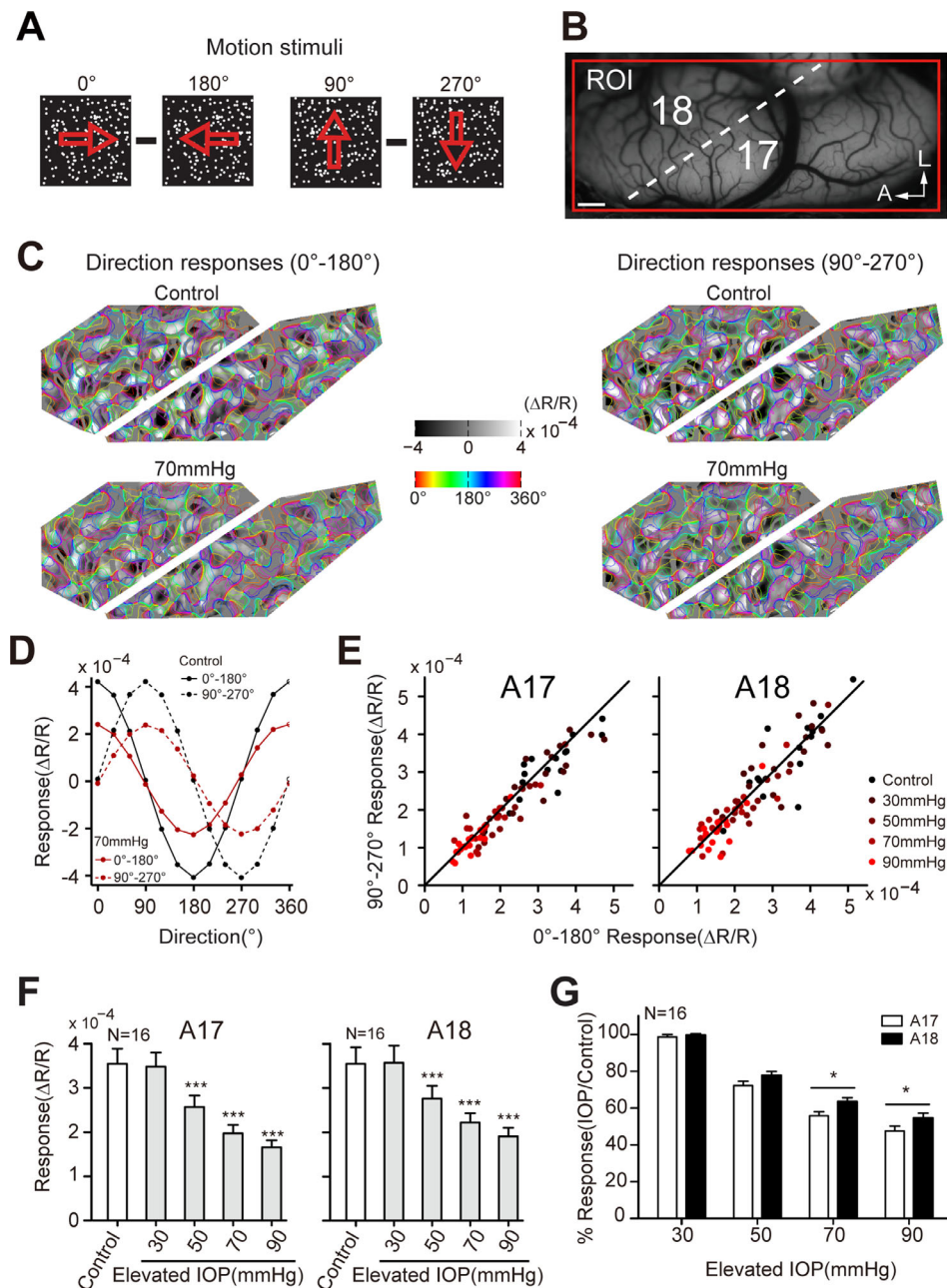


**FIGURE 3.** Cortical population responses to different motion directions during acute IOP elevation across animals. **(A)** Stimuli used for activating distinct direction selective responses. **(B)** The cortical vasculature of areas 17 and 18. A, anterior; L, lateral. Scale bar, 1 mm. **(C)** Differential population response maps for opponent directions 0° versus 180°, and 90° versus 270°, each with superimposed iso-contours for direction preference, at normal IOP and IOP at 70 mm Hg. **(D)** The direction selective response curves for area 17 derived from the population responses in **(C)**. Solid and broken lines represent different motion directions; black and red represent control and 70 mm Hg IOP conditions, respectively. **(E)** Comparison of the differential cortical response to 0° and 180° directions with that to 90° and 270° directions; each point represents a single eye, replicated across a control plus four IOP conditions. **(F)** Comparison of the average cortical responses during each IOP elevation with the control condition. Controls were taken as cortical responses before each acute IOP elevation. No significant differences in response amplitude were observed among the controls for each IOP condition (area 17:  $F = 0.02$ ,  $P = 0.99$ ; area 18:  $F = 0.20$ ,  $P = 0.89$ ; 1-way ANOVA). A17, area 17; A18, area 18. **(G)** Comparison of the response ratio between areas 17 and 18 at each acutely elevated IOP level. \* $P < 0.05$ ; \*\*\* $P < 0.001$ .  $N = 16$  eyes. Error bar denotes SEM. ROI, region of interest.

## DISCUSSION

Although deficits in motion perception have been identified in chronic glaucoma,<sup>5</sup> it remains unknown how far motion, or spatiotemporal processing in general, is affected during the acute phase of IOP attack. In the present study, we physi-

ologically characterized the impact of acute IOP elevation on cortical motion direction and orientation responses by simultaneous intrinsic signal optical imaging of cat visual areas 17 and 18. During precise reversible modulations of IOP elevations, we found cortical responses specific to motion direction were significantly suppressed at IOP levels of 50

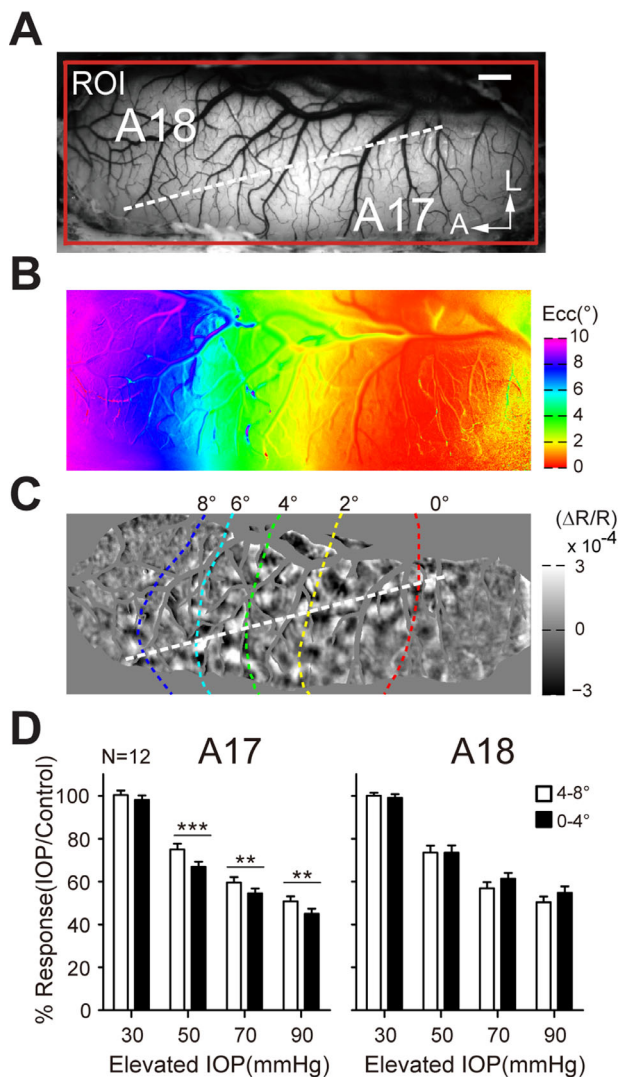


**FIGURE 4.** Cortical responses at different retinal eccentricities during acute IOP elevation. (A) The cortical surface displaying areas 17 and 18 and their border, indicated by the white dashed line. A17, area 17; A18, area 18; A, anterior; L, lateral. Scale bar, 1 mm. (B) Retinal eccentricity map of the cortical surface in areas 17 and 18. (C) Cortical population responses, as shown by a differential map for direction with superimposed iso-eccentricity contours according to the eccentricity map in (B). (D) Comparison of the response ratio of cortical direction maps between central ( $0^{\circ}$ – $4^{\circ}$ ) and peripheral ( $4^{\circ}$ – $8^{\circ}$ ) retinal visual fields at each acutely elevated IOP level.  $***P < 0.001$ ;  $**P < 0.01$ .  $N = 12$  eyes. Error bar denotes SEM. ROI, region of interest.

mm Hg and above in both areas 17 and 18. This response suppression was most profound for central visual field of area 17 ( $0^{\circ}$ – $4^{\circ}$ ), lessening into paracentral visual field ( $4^{\circ}$ – $8^{\circ}$ ), and into adjacent area 18. However, in all these cortical regions, the magnitude of motion response suppression was exceeded by the level of suppression that we recorded for orientation. Together, the topographic pattern and feature specificity of these effects imply a pathway-specific impairment of visual function during acute IOP elevation.

In felines, two pathways (X and Y) are clearly distinguishable by both anatomic and physiological criteria. In general, X retinal ganglion cells correspond to the morphologically identified  $\beta$  class with the smallest dendritic

fields, correspondingly small receptive fields, and broadly linear responses. Y retinal ganglion cells pertain to  $\alpha$  class with large dendritic fields that respond in a more nonlinear fashion within their receptive field.<sup>20,38,39</sup> Broadly, X cells respond to higher spatial frequencies at low temporal frequencies, whereas Y cells respond to low spatial frequency and possess high temporal sensitivity.<sup>40,41</sup> All X and Y cells innervate the LGN, a subcortical relay nucleus, before projecting to visual cortex. LGN X cells send projections exclusively to area 17, whereas LGN Y cells innervate both areas 17 and 18.<sup>28,42</sup> As a result, neurons in areas 17 and 18 show distinct spatial and temporal response tuning properties.<sup>43</sup> This evidence supports the common view that the dominant input to area 17 is from the X-cell pathway, and the dominant input to area 18 is from the Y-cell pathway.<sup>22,44</sup> Previous studies have ascertained that acute IOP elevation preferentially disrupts the function of X cells in both retina and LGN of cats,<sup>45,46</sup> and, clearly, our observation that area 17 motion responses are suppressed more than those of area 18 is concordant with this finding. Indeed, the response suppression in area 18 must be due, in part, to a reduced (largely X-dependent) input from area 17, given that transient inactivation of area 17 is reported to reduce both general responsivity and directional selectivity in area 18.<sup>47</sup>

Two further aspects of our findings support the contention that acute elevation of IOP has a more severe effect on X than Y pathway activity. First, the differential suppression of motion responses in central and paracentral field in area 17 reflects the changes in the relative frequency of X and Y cells in the retina. The X-cell pathway is numerically dominant, outnumbering Y cells by approximately 60:1 at the point of minimal Y-cell density, the center of the area centralis<sup>48</sup>; given some variance in reported cell-counts of cat retina, we estimate that this ratio falls to approximately 30:1 and 15:1, respectively, for the  $0^{\circ}$ – $4^{\circ}$  and  $4^{\circ}$ – $8^{\circ}$  eccentricities that we examined.<sup>48–51</sup> Second, we found that the differential activation in respect of orthogonally oriented gratings was more suppressed than that associated with opposite directions of dot motion, as measured in the same preparation at the same level of IOP elevation. This result accords with the outcome of a previous study using a similar methodology, in which brief IOP elevation (80 mm Hg, 4 minutes) caused maximal degradation of orientation maps when high frequency gratings were used to stimulate the posterior section of area 17 (central visual field).<sup>27</sup> These authors also inferred that X pathway function was the more severely compromised.

In primate retina, parasol, and midget ganglion cells, respectively, project to the two magnocellular and four parvocellular layers of the LGN. Morphologically and physiologically, magnocellular and parvocellular cells of primates are held to be functionally analogous to X and Y cells in cats,<sup>52,53</sup> and their retinal distributions are also similar: the density of both magnocellular and parvocellular ganglion cells is highest in central visual field and falls toward the periphery, but the proportion of parvocellular ganglion cells in relation to all ganglion cells declines with eccentricity, whereas that of magnocellular ganglion cells rises.<sup>54,55</sup> Histopathological assessment of the consequences of chronic IOP elevation in glaucoma patients and nonhuman primates reported selective damage to the magnocellular pathway.<sup>56–59</sup> Correspondingly, a wealth of studies have proposed sensitivity tests for early glaucoma detection based on magnocellular dysfunction. Some studies reported visual motion deficits solely in peripheral visual field locations,<sup>32,33</sup>

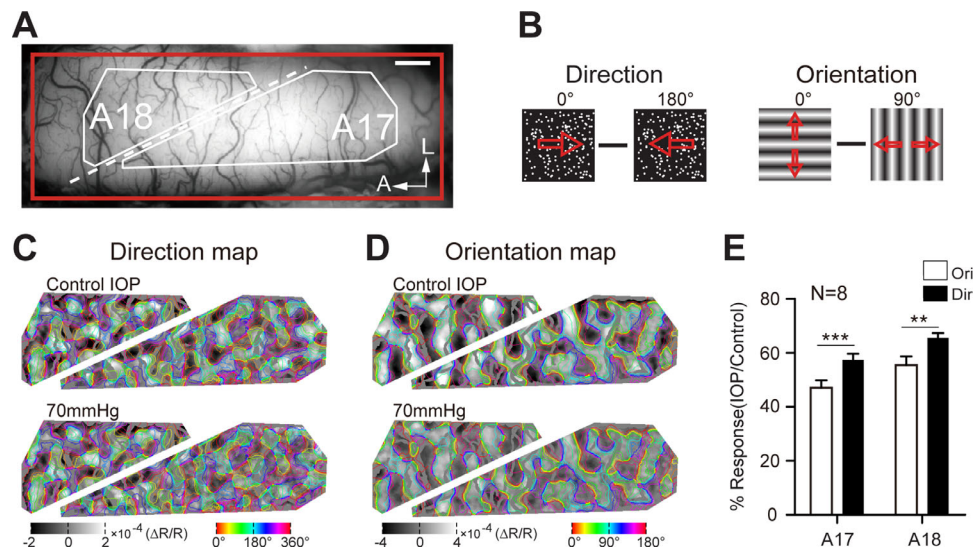


**FIGURE 5.** Cortical differential response maps for direction and orientation during acute IOP elevation. (A) Cortical surface of areas 17 and 18 adjoining their border, indicated by the *white dashed line*. A17, area 17; A18, area 18; A, anterior; L, lateral. *Scale bar*, 1 mm. (B) Stimuli used for activating cortical direction and orientation population responses. (C) Differential population response maps for direction with superimposed iso-contours for direction preference. (D) Differential population response maps for orientation with superimposed iso-contours for orientation preference. (E) Comparison of the response ratios (IOP elevation to control) for cortical population responses to direction and orientation in areas 17 and 18. \*\*\* $P < 0.001$ ; \*\* $P < 0.01$ .  $N = 8$  eyes. *Error bar* denotes SEM.

whereas a number of others—using a variety of stimuli and protocols sensitive to magnocellular deficits—have reported elevated motion thresholds in central visual field.<sup>8,9,60–62</sup> Notwithstanding these findings, the selective degradation of magnocellular function by chronic IOP elevation has been called into question. Although some studies continue to support this view,<sup>63–66</sup> many others, both histological<sup>67,68</sup> and psychophysical,<sup>6,69–74</sup> do not. A recent assessment of chronic primary open angle glaucoma patients (on which all these studies have focused exclusively) is that central and peripheral sites of early glaucomatous damage are equally efficiently detected by luminance perimetry with a 2° grid, as used in conjunction with optical coherence tomography scans.<sup>75</sup> To date, only one study has examined the immediate effects of acute IOP elevations on cortical responses in nonhuman primates (macaque monkeys) and found that central vision with higher acuities at smaller eccentricities is more severely impaired, implicating relatively greater dysfunction in the parvocellular pathway.<sup>76</sup> The motion response suppression in felines reported here, affecting area 17 more than area 18, suggests that acute IOP attacks cause more disruption to the X pathways for motion processing.

Although the analysis of motion through direction-selective mechanisms is primarily associated with magnocellular and Y-cell pathways in primates and carnivores,<sup>52</sup> this is not necessarily an exclusive relationship. Monkeys retain the capacity to discriminate direction (albeit at higher contrast) following geniculate inactivation of magnocellular function.<sup>77</sup> In a similar vein, monocular blockade of Y fibers in the optic nerve (by means of a pressure cuff) has little effect on direction or speed tuning in area 17 of cats; area 18 shows a more marked reduction in optimal speed but, again, little change in direction selectivity.<sup>52,78,79</sup> In general, there is no neurophysiological basis to discount a role for the most fine grained pathway (X cell or parvocellular) in motion perception. For human vision, generalizing periph-

eral psychophysical findings to the entire visual field, the parvocellular system appears to determine the threshold for motion acuity (the smallest displacement whose direction can be discriminated).<sup>80</sup>

Chronic IOP elevation may eventually lead to neuron death, not only in the retina but also in LGN and visual cortex.<sup>81,82</sup> Distinct from conditions in chronic glaucoma, the IOP modulations in the current study are transient and reversible. The depression of visual responses in both retina and visual cortex can be compensated by modulation of perfusion pressure during acute IOP elevation.<sup>83</sup> It is also reported that a moderate-level IOP elevation (~35 mm Hg) could induce abnormal high electroretinogram (ERG), whereas the visual evoked potential (VEP) components appeared attenuated until the IOP exceeds 70 mm Hg above the diastolic BP.<sup>84</sup> Selective decrease of ganglion cells and synapses were observed in mouse retina after transient ocular hypertension.<sup>85</sup> The present study revealed that acute IOP elevation at 50 mm Hg and above could significantly decrease the amplitude of cortical motion direction responses without changing neurons' direction preferences. The differential depressive impacts on cortical responses of visual motion direction and orientation by acute IOP attacks suggest that the sensitivity of physiological examination may not only depend on elevated IOP levels, but also on specific visual features or stimuli tested.

## CONCLUSIONS

The present study directly examines the cortical population responses to motion direction within and between early visual cortices of the same preparation during the acute phase of IOP elevation. We demonstrate that cortical motion responses are substantially depressed in both areas 17 and 18, especially in central visual field locations of area 17. Our results indicate that distinct cell-type-specific pathways are differentially impacted by acute IOP elevation, and provides



direct neural evidence underlying visual deficits in motion perception of acute glaucoma patients, particularly in the central visual field.

### Acknowledgments

Supported by the National Natural Science Foundation of China (No. 81430007 [XHS], No. 81790641 [XHS], and No. 31600846 [NNY]); the Shanghai Municipal Science and Technology Major Project (No. 2018SHZDZX05 [WW]); the Strategic Priority Research Program of Chinese Academy of Sciences (No. XDB32060200 [WW]); the Shanghai Committee of Science and Technology (No. 17410712500 [XHS]); and the Top Priority of Clinical Medicine Center of Shanghai (No. 2017ZZ01020 [XHS]). The funders had no role in study design, data collection and analysis, decision to publish, or preparation of the manuscript.

Disclosure: **N. Yuan**, None; **M. Li**, None; **X. Chen**, None; **Y. Lu**, None; **Y. Fang**, None; **H. Gong**, None; **L. Qian**, None; **J. Wu**, None; **S. Zhang**, None; **S. Shipp**, None; **I.M. Andolina**, None; **X. Sun**, None; **W. Wang**, None

### References

- Jonas JB, Aung T, Bourne RR, Bron AM, Ritch R, Panda-Jonas S. Glaucoma. *Lancet*. 2017;390:2183–2193.
- Quigley HA. Glaucoma. *Lancet*. 2011;377:1367–1377.
- Sun X, Dai Y, Chen Y, et al. Primary angle closure glaucoma: what we know and what we don't know. *Prog Retin Eye Res*. 2017;57:26–45.
- Weinreb RN, Leung CK, Crowston JG, et al. Primary open-angle glaucoma. *Nat Rev Dis Primers*. 2016;2:16067.
- Shabana N, Cornilleau Peres V, Carkeet A, Chew PT. Motion perception in glaucoma patients: a review. *Surv Ophthalmol*. 2003;48:92–106.
- Ansari EA, Morgan JE, Snowden RJ. Psychophysical characterisation of early functional loss in glaucoma and ocular hypertension. *Br J Ophthalmol*. 2002;86:1131–1135.
- Falkenberg HK, Bex PJ. Sources of motion-sensitivity loss in glaucoma. *Invest Ophthalmol Vis Sci*. 2007;48:2913–2921.
- Sahraie A, Barbur JL, Edgar DF, Weiskrantz L. Motion discrimination of single targets: comparison of preliminary findings in normal subjects and patients with glaucoma. *Graefes Arch Clin Exp Ophthalmol*. 1996;234:553–560.
- Tyler CW. Specific deficits of flicker sensitivity in glaucoma and ocular hypertension. *Invest Ophthalmol Vis Sci*. 1981;20:204–212.
- Montana CL, Bhorade AM. Glaucoma and quality of life: fall and driving risk. *Curr Opin Ophthalmol*. 2018;29:135–140.
- Razeghinejad MR, Myers JS. Contemporary approach to the diagnosis and management of primary angle-closure disease. *Surv Ophthalmol*. 2018;63:754–768.
- Prum BE, Jr., Herndon LW, Jr., Moroi SE, et al. Primary Angle Closure Preferred Practice Pattern(R) Guidelines. *Ophthalmology*. 2016;123:P1–P40.
- Shmuel A, Grinvald A. Functional organization for direction of motion and its relationship to orientation maps in cat area 18. *J Neurosci*. 1996;16:6945–6964.
- An X, Gong HL, McLoughlin N, Yang YP, Wang W. The mechanism for processing random-dot motion at various speeds in early visual cortices. *PLoS One*. 2014;9:e93115.
- Galuske RA, Schmidt KE, Goebel R, Lomber SG, Payne BR. The role of feedback in shaping neural representations in cat visual cortex. *Proc Natl Acad Sci U S A*. 2002;99:17083–17088.
- Kisvarday ZF, Buzas P, Eysel UT. Calculating direction maps from intrinsic signals revealed by optical imaging. *Cereb Cortex*. 2001;11:636–647.
- Ribot J, Tanaka S, O'Hashi K, Ajima A. Anisotropy in the representation of direction preferences in cat area 18. *Eur J Neurosci*. 2008;27:2773–2780.
- Swindale NV, Grinvald A, Shmuel A. The spatial pattern of response magnitude and selectivity for orientation and direction in cat visual cortex. *Cereb Cortex*. 2003;13:225–238.
- Lu HD, Chen G, Tanigawa H, Roe AW. A motion direction map in macaque V2. *Neuron*. 2010;68:1002–1013.
- Boycott BB, Wässle H. The morphological types of ganglion cells of the domestic cat's retina. *J Physiol*. 1974;240:397–419.
- Boyd JD, Matsubara JA. Laminar and columnar patterns of geniculocortical projections in the cat: relationship to cytochrome oxidase. *J Comp Neurol*. 1996;365:659–682.
- Sherman SM. Parallel W-, X- and Y-cell pathways in the cat: a model for visual function. In: Rose D, Dobson VG, eds. *Models of the Visual Cortex*. Hoboken, NJ: Wiley; 1985:71–84.
- Lu Y, Yin J, Chen Z, et al. Revealing detail along the visual hierarchy: neural clustering preserves acuity from V1 to V4. *Neuron*. 2018;98:417–428.e3.
- Grozdanic SD, Matic M, Betts DM, Sakaguchi DS, Kardon RH. Recovery of canine retina and optic nerve function after acute elevation of intraocular pressure: implications for canine glaucoma treatment. *Vet Ophthalmol*. 2007;10:101–107.
- Vanni MP, Provost J, Lesage F, Casanova C. Evaluation of receptive field size from higher harmonics in visuotopic mapping using continuous stimulation optical imaging. *J Neurosci Meth*. 2010;189:138–150.
- Pan Y, Chen M, Yin J, et al. Equivalent representation of real and illusory contours in macaque V4. *J Neurosci*. 2012;32:6760–6770.
- Chen X, Sun C, Huang L, Shou T. Selective loss of orientation column maps in visual cortex during brief elevation of intraocular pressure. *Invest Ophthalmol Vis Sci*. 2003;44:435–441.
- Humphrey AL, Sur M, Uhlrich DJ, Sherman SM. Termination patterns of individual X- and Y-cell axons in the visual cortex of the cat: projections to area 18, to the 17/18 border region, and to both areas 17 and 18. *J Comp Neurol*. 1985;233:190–212.
- Humphrey AL, Sur M, Uhlrich DJ, Sherman SM. Projection patterns of individual X- and Y-cell axons from the lateral geniculate nucleus to cortical area 17 in the cat. *J Comp Neurol*. 1985;233:159–189.
- Ahmed B, Hammond P. Response of cat retinal ganglion cells to motion of visual texture. *Exp Brain Res*. 1984;53:444–450.
- Mason R. Responses of cells in the dorsal lateral geniculate complex of the cat to textured visual stimuli. *Exp Brain Res*. 1976;25:323–326.
- Bosworth CF, Sample PA, Gupta N, Bathija R, Weinreb RN. Motion automated perimetry identifies early glaucomatous field defects. *Arch Ophthalmol*. 1998;116:1153–1158.
- Joffe KM, Raymond JE, Chrichton A. Motion coherence perimetry in glaucoma and suspected glaucoma. *Vision Res*. 1997;37:955–964.
- Albus K, Beckmann R. Second and third visual areas of the cat: interindividual variability in retinotopic arrangement and cortical location. *J Physiol*. 1980;299:247–276.
- Tusa RJ, Palmer LA, Rosenquist AC. The retinotopic organization of area 17 (striate cortex) in the cat. *J Comp Neurol*. 1978;177:213–235.
- Tusa RJ, Rosenquist AC, Palmer LA. Retinotopic organization of areas 18 and 19 in the cat. *J Comp Neurol*. 1979;185:657–678.

37. Pasternak T, Horn K. Spatial vision of the cat: variation with eccentricity. *Vis Neurosci.* 1991;6:151–158.
38. Stone J, Fukuda Y. Properties of cat retinal ganglion cells: a comparison of W-cells with X- and Y-cells. *J Neurophysiol.* 1974;37:722–748.
39. Cleland BG, Dubin MW, Levick WR. Sustained and transient neurones in the cat's retina and lateral geniculate nucleus. *J Physiol.* 1971;217:473–496.
40. Cleland BG, Harding TH, Tulunay-Keeseey U. Visual resolution and receptive field size: examination of two kinds of cat retinal ganglion cell. *Science.* 1979;205:1015–1017.
41. Victor JD, Shapley RM. Receptive-field mechanisms of cat X and Y retinal ganglion-cells. *J Gen Physiol.* 1979;74:275–298.
42. Stone J, Dreher B. Projection of X- and Y-cells of the cat's lateral geniculate nucleus to areas 17 and 18 of visual cortex. *J Neurophysiol.* 1973;36:551–567.
43. Movshon JA, Thompson ID, Tolhurst DJ. Spatial and temporal contrast sensitivity of neurones in areas 17 and 18 of the cat's visual cortex. *J Physiol.* 1978;283:101–120.
44. Stone J, Dreher B, Leventhal A. Hierarchical and parallel mechanisms in the organization of visual cortex. *Brain Res.* 1979;180:345–394.
45. Zhou Y, Wang W, Ren B, Shou T. Receptive field properties of cat retinal ganglion cells during short-term IOP elevation. *Invest Ophthalmol Vis Sci.* 1994;35:2758–2764.
46. Shou TD, Zhou YF. Y-cells in the cat retina are more tolerant than X-cells to brief elevation of IOP. *Invest Ophthalmol Vis Sci.* 1989;30:2093–2098.
47. Casanova C, Michaud Y, Morin C, McKinley PA, Molotchnikoff S. Visual responsiveness and direction selectivity of cells in area 18 during local reversible inactivation of area 17 in cats. *Vis Neurosci.* 1992;9:581–593.
48. Stein JJ, Johnson SA, Berson DM. Distribution and coverage of beta cells in the cat retina. *J Comp Neurol.* 1996;372:597–617.
49. Fukuda Y, Stone J. Retinal distribution and central projections of Y-, X-, and W-cells of the cat's retina. *J Neurophysiol.* 1974;37:749–772.
50. Leventhal AG. Morphology and distribution of retinal ganglion cells projecting to different layers of the dorsal lateral geniculate nucleus in normal and Siamese cats. *J Neurosci.* 1982;2:1024–1042.
51. Stone J. The number and distribution of ganglion cells in the cat's retina. *J Comp Neurol.* 1978;180:753–771.
52. Burke W, Dreher B, Wang C. Selective block of conduction in Y optic nerve fibres: significance for the concept of parallel processing. *Eur J Neurosci.* 1998;10:8–19.
53. Shapley R, Perry VH. Cat and monkey retinal ganglion-cells and their visual functional roles. *Trends Neurosci.* 1986;9:229–235.
54. Dacey DM. Physiology, morphology and spatial densities of identified ganglion-cell types in primate retina. *Ciba F Symp.* 1994;184:12–28.
55. Silveira LCL, Perry VH. The topography of magnocellular projecting ganglion-cells (M-ganglion cells) in the primate retina. *Neuroscience.* 1991;40:217–237.
56. Dandona L, Hendrickson A, Quigley HA. Selective effects of experimental glaucoma on axonal transport by retinal ganglion cells to the dorsal lateral geniculate nucleus. *Invest Ophthalmol Vis Sci.* 1991;32:1593–1599.
57. Glovinsky Y, Quigley HA, Dunkelberger GR. Retinal ganglion-cell loss is size dependent in experimental glaucoma. *Invest Ophthalmol Vis Sci.* 1991;32:484–491.
58. Quigley HA, Sanchez RM, Dunkelberger GR, L'Hernault NL, Baginski TA. Chronic glaucoma selectively damages large optic nerve fibers. *Invest Ophthalmol Vis Sci.* 1987;28:913–920.
59. Kerrigan-Baumrind LA, Quigley HA, Pease ME, Kerrigan DF, Mitchell RS. Number of ganglion cells in glaucoma eyes compared with threshold visual field tests in the same persons. *Invest Ophthalmol Vis Sci.* 2000;41:741–748.
60. Bullimore MA, Wood JM, Swenson K. Motion perception in glaucoma. *Invest Ophthalmol Vis Sci.* 1993;34:3526–3533.
61. Karwatsky P, Bertone A, Overbury O, Faubert J. Defining the nature of motion perception deficits in glaucoma using simple and complex motion stimuli. *Optom Vis Sci.* 2006;83:466–472.
62. Westcott MC, Fitzke FW, Hitchings RA. Abnormal motion displacement thresholds are associated with fine scale luminance sensitivity loss in glaucoma. *Vision Res.* 1998;38:3171–3180.
63. Anderson RS, O'Brien C. Psychophysical evidence for a selective loss of M ganglion cells in glaucoma. *Vision Res.* 1997;37:1079–1083.
64. Sun H, Swanson WH, Arvidson B, Dul MW. Assessment of contrast gain signature in inferred magnocellular and parvocellular pathways in patients with glaucoma. *Vision Res.* 2008;48:2633–2641.
65. Weber AJ, Chen H, Hubbard WC, Kaufman PL. Experimental glaucoma and cell size, density, and number in the primate lateral geniculate nucleus. *Invest Ophthalmol Vis Sci.* 2000;41:1370–1379.
66. Zhang P, Wen W, Sun X, He S. Selective reduction of fMRI responses to transient achromatic stimuli in the magnocellular layers of the LGN and the superficial layer of the SC of early glaucoma patients. *Hum Brain Mapp.* 2016;37:558–569.
67. Morgan JE, Uchida H, Caprioli J. Retinal ganglion cell death in experimental glaucoma. *Brit J Ophthalmol.* 2000;84:303–310.
68. Yucel YH, Zhang Q, Gupta N, Kaufman PL, Weinreb RN. Loss of neurons in magnocellular and parvocellular layers of the lateral geniculate nucleus in glaucoma. *Arch Ophthalmol.* 2000;118:378–384.
69. Battista J, Badcock DR, McKendrick AM. Spatial summation properties for magnocellular and parvocellular pathways in glaucoma. *Invest Ophthalmol Vis Sci.* 2009;50:1221–1226.
70. Greenstein VC, Halevy D, Zaidi Q, Koenig KL, Ritch RH. Chromatic and luminance systems deficits in glaucoma. *Vision Res.* 1996;36:621–629.
71. Martin L, Wanger P, Vancea L, Gothlin B. Concordance of high-pass resolution perimetry and frequency-doubling technology perimetry results in glaucoma: no support for selective ganglion cell damage. *J Glaucoma.* 2003;12:40–44.
72. McKendrick AM, Badcock DR, Morgan WH. Psychophysical measurement of neural adaptation abnormalities in magnocellular and parvocellular pathways in glaucoma. *Invest Ophthalmol Vis Sci.* 2004;45:1846–1853.
73. McKendrick AM, Badcock DR, Morgan WH. The detection of both global motion and global form is disrupted in glaucoma. *Invest Ophthalmol Vis Sci.* 2005;46:3693–3701.
74. McKendrick AM, Sampson GP, Walland MJ, Badcock DR. Contrast sensitivity changes due to glaucoma and normal aging: low-spatial-frequency losses in both magnocellular and parvocellular pathways. *Invest Ophthalmol Vis Sci.* 2007;48:2115–2122.
75. Hood DC, Tsamis E, Bommakanti NK, et al. Structure-function agreement is better than commonly thought in eyes with early glaucoma. *Invest Ophthalmol Vis Sci.* 2019;60:4241–4248.
76. Li M, Yuan N, Chen X, et al. Impact of acute intraocular pressure elevation on the visual acuity of non-human primates. *EBioMedicine.* 2019;44:554–562.

77. Merigan WH, Byrne CE, Maunsell JHR. Does primate motion perception depend on the magnocellular pathway? *J Neurosci*. 1991;11:3422–3429.
78. Burke W, Dreher B, Michalski A, Cleland BG, Rowe MH. Effects of selective pressure block of Y-type optic nerve fibers on the receptive-field properties of neurons in the striate cortex of the cat. *Vis Neurosci*. 1992;9:47–64.
79. Dreher B, Michalski A, Cleland BG, Burke W. Effects of selective pressure block of Y-type optic nerve fibers on the receptive-field properties of neurons in area 18 of the visual cortex of the cat. *Vis Neurosci*. 1992;9:65–78.
80. Anderson SJ, Drasdo N, Thompson CM. Parvocellular neurons limit motion acuity in human peripheral vision. *Proc R Soc Lond B Biol Sci*. 1995;261:129–138.
81. Nuzzi R, Dallorto L, Rolle T. Changes of visual pathway and brain connectivity in glaucoma: a systematic review. *Front Neurosci*. 2018;12:363.
82. Shou T, Liu J, Wang W, Zhou Y, Zhao K. Differential dendritic shrinkage of alpha and beta retinal ganglion cells in cats with chronic glaucoma. *Invest Ophthalmol Vis Sci*. 2003;44:3005–3010.
83. Grehn F, Prost M. Function of retinal nerve fibers depends on perfusion pressure: neurophysiologic investigations during acute intraocular pressure elevation. *Invest Ophthalmol Vis Sci*. 1983;24:347–353.
84. Uenoyama K, McDonald JS, Drance SM. The effect of intraocular pressure on visual electrical responses. *Arch Ophthalmol*. 1969;81:722–729.
85. Ou Y, Jo RE, Ullian EM, Wong RO, Della Santina L. Selective vulnerability of specific retinal ganglion cell types and synapses after transient ocular hypertension. *J Neurosci*. 2016;36:9240–9252.